Investigation on mechanical, electrical and morphological of high-density polyethylene (HDPE) reinforced with different particle size and composition of graphene nanoplatelets (GNP)

W. M. W. Mohammad, E. A. G. E. Ali*, M. A. A. Abdullah, C. K. Sheng
Faculty of Science and Marine Environment, Universiti Malaysia Terengganu, 21030 Kuala Nerus, Terengganu, Malaysia

Graphene nanoplatelets (GNP) are just one of the attractive graphene-based nanomaterials that are rapidly emerging and have sparked the interest of many industries. These small stacks of platelet-shaped graphene sheets have a unique size and morphology that quickly disperse into other materials such as polymers, resulting in higher-value composite materials with improved thermal, conductivity, and mechanical capabilities. A detailed analysis of reinforced High-Density Polyethylene (HDPE) using different sizes (2, 15, 25 μm) and compositions (8, 10, 15 wt.%) of Graphene Nanoplatelets (GNP) has been conducted. The microstructure of the HDPE/GNP nanocomposites was extensively examined during the melt blending and injection moulding processes. Based on the results, the nanocomposites with different sizes of GNP exhibited dissimilar behaviour with different compositions. Furthermore, scanning electron microscope (SEM) results indicated a homogeneous dispersion for GNP in melt mixing. Moreover, thermogravimetric (TG) data demonstrate that increasing filler showed a slight increase in the material's thermal stability. The use of GNP improved mechanical properties, as evidenced by the increases in Young's modulus of yield strength from around 100 MPa to over 400 MPa. This study provides a practical reference for the industrial preparation of polymer-based graphene nanocomposites.

(Received September 26, 2023; Accepted January 4, 2024)

Keywords: Graphene nano-platelets, High-density polyethylene, Thermal properties, Mechanical properties, Morphology

1. Introduction

A new class of nanostructures has evolved because of advancements in nanoscience, which have made the creation of novel technologies extremely desirable. Graphene, also known as the "mother of all graphitic forms," has become one of the most promising nanomaterials due to a unique combination of exceptional properties. The mechanical cleavage of graphite using adhesive tape showcased the ability to produce individual layers of graphene, which is not only exceptionally thin but also remarkably strong. Moreover, graphene exhibits excellent heat and electrical conductivity, surpassing all other materials in these aspects [1]. The name "graphene" refers to a single layer of carbon atoms that are closely clustered together within a benzene-ring structure. Numerous carbon-based materials, including graphite, massive fullerenes, and nanotubes, are widely used to characterise its properties [2]. Due to its small size and unique 2D-atomic crystal, graphene exhibits outstanding physical and chemical features, such as enhanced surface area, molar extinction coefficients, adjustable capabilities, quantum effects, and magnetic and optical properties. Many researchers are intrigued in carbon-based nanomaterials because they offer unique thermodynamic, biomechanical, electrical, optical, and structural properties [3]. Graphene and its derivatives, including graphene nanoplatelets (GNP), graphene oxide (GO), reduced GO (rGO), and functionalized GO (FGO), possess exceptional properties such as a large surface area, high Young's modulus, enhanced electron mobility, and excellent thermal conductivity. These derivatives, while sharing similarities with graphene, also exhibit distinct qualities and characteristics that make them

* Corresponding author: engku_ghapur@umt.edu.my
https://doi.org/10.15251/DJNB.2024.191.41

widely utilized in various applications. [4]. These carbon-based fillers have significant electrical conductivities, and when they are nanoscale, their high surface-to-volume ratio allows for exceptionally high conductivities [5].

In contrast to other carbon nanomaterial, graphene nanoplatelets (GNP) have drawn interest since they can be produced in large quantities and can be taken into consideration when creating polymer nanocomposites [6]. Since their main characteristics are light weight, high aspect ratio with planar shape, good mechanical properties, excellent thermal and electrical conductivities, along with low cost and easy manufacture, GNP have a wide range of applications as standalone materials, neat coatings, and fillers of composites [7]. After mixing with glass fibres, polymers, or another matrix, GNP can offer significant conductivity due to the high interfacial interaction of nanoplates with the matrices [8]. In addition, GNP can improve the mechanical properties of various composites, such as stiffness and tensile strength.

Polymers are renowned for being effective insulators due to their poor thermal and electrical conductivity. Therefore, extensive research has been carried out to enhance the mechanical and thermal properties as well as boost the electrical conductivity by incorporating conductive nanofillers into thermoplastic resins since it can produce innovative functionality [9]. The conductive composites are composites with significant electrical conductivity when conductive filler such as graphene nanoplatelets is added to a non-conductive (or less conductive) matrix such as a polymer, which can result in the so-called electrically conductive composites that exhibit a wide range of electrical conductivities [10]. High-density polyethylene (HDPE) was utilised as a matrix for the nanofillers of the graphene nanoplatelets to improve the electrical and mechanical capabilities of the nanocomposite [11]. It is also regarded as one of the most frequently used thermoplastic polymers due to its exceptional properties, such as regular chain structure, excellent chemical inertness, combination of low energy requirements for processing and low cost, moisture absorption close to zero, and excellent biocompatibility. Additionally, it is relatively lightweight and can withstand moisture, abrasion, and corrosion. It has many uses in the agricultural, gas pipeline manufacturing, food packaging, and service sectors [12].

In this work, high-density polyethylene (HDPE) containing GNP nanocomposites were fabricated using melt mixing method followed by injection moulding. The melt blending approach has the advantages of being more environmentally friendly (solvent free), more productive, and simpler to scale to industrial levels [13]. The prime aim of this study is to produce HDPE/GNP nanocomposites with high flexibility, tensile strength, electrical, thermal, and mechanical properties at low cost.

2. Experimental

2.1. Materials

A commercial high-density polyethylene (HDPE) in the form of pellets were provided by Polyethylene Malaysia Sdn. Bhd. was used as a matrix material. Graphene nanoplatelets (GNP) were procured from Aldrich and three different sizes (2 μm, 15 μm, and 25 μm) were used. The physical properties of graphene nanoplatelets data are presented in Table 1.

2.2. Preparation of HDPE/GNP polymer nanocomposites

Preparation of HDPE/GNP nanocomposites involved a melt mixing approach with varying GNP content (8%, 10%, and 15%). The mixture was processed in a Haake Internal Mixer equipped with a rotor blade operating at 50 rpm and at temperature of 180°C for 10 minutes. Injection moulding was used to produce tensile bar-shaped specimens, using a Haake MiniJet II following ASTM standard D638.

Table 1. Characteristics of GNP as a filler.

GNP	Particle size (μm)	Concentrations of GNP (wt%)	Name of sample	Surface Area (m^2/g)
G1	2	8%	8 wt% G1	300
		10%	10wt% G1	
		15%	15wt% G1	
G2	15	8%	8 wt% G2	120-150
		10%	10wt% G2	
		15%	15wt% G2	
G3	25	8%	8 wt% G3	50-80
		10%	10wt% G3	
		15%	15wt% G3	

2.3. Characterizations

The morphology structure of HDPE/GNP nanocomposites was examined using scanning electron microscope from TESCAN model VEGA. Cross-sectional samples of the composite were taken after tensile testing. The thermogravimetric analysis was carried out using Mettler Toledo (Model TGA/DSC1) in an inert atmosphere of argon with a heating rate 10 ml/min starting from room temperature and ending at 700°C. Fourier Transform Infrared (FTIR) spectrometer (Bruker Invenio-S) was used to identify changes in chemical functional groups by using thin KBr (potassium bromide) disc method. For each sample, the analysis was carried out at a wavenumber ranging from 400 cm^{-1} to 4000 cm^{-1}. The HDPE/GNP composites were evaluated for their ability to resist deformation and fracture under applied loads at room temperature using two standardized tests. The first test, which measured the composites' tensile properties, was conducted using an Instron 4301 universal testing machine in accordance with ASTM D638-10 at a crosshead speed of 10 mm/min. The second test, the Izod impact test, was performed using notched specimens with 11 J pendulum, and as per ASTM D256-10 guidelines. These tests were selected because they primarily assess a material's ability to resist deformation and fracture under applied loads, particularly at normal ambient temperatures. The electrical conductivity was measured using the 2-point probe method using a Keithley electrometer (Model 2400). The sheet's electrical conductivity (σ) was calculated using the following formula:

$$\sigma = \left(\frac{t}{R_v} \times A\right)$$

where t and A are the sheet's thickness and effective area of the measuring electrodes, respectively, and R is the sample's resistance.

3. Results and discussion

3.1. Thermogravimetric Analysis (TGA)

Figure 1 displays test sample TGA profiles as a function of temperature. TGA curves reveal that all samples exhibited similar thermal behaviours. The samples begin to degrade at temperatures between about 300° - 500 °C and this causes the decomposition of the polymer matrix [14]. The gradual decrease in weight is due to the protective effect provided by the GNP layer on the HDPE surface, and this protection diminishes at higher temperatures [15]. It reveals that during the primary weight loss phase, the involvement of oxygen speeds up the degradation of both pure HDPE and HDPE/GNP composite materials through decomposition mechanisms. As shown in Table 1, there has been an improvement in the thermal stability of the composites reinforced with GNP. The stable inorganic phase of GNP is associated with an increase in degradation temperature, indicating strong interactions between the filler and the polymer matrix (HDPE/GNP) [16]. It is demonstrated that the thermal stability of HDPE/GNP is dependent on GNP loading, as it is showing a drastically increase

with increasing GNP loading. The HDPE/GNP composite with large particle size and high concentration shows having better thermal stability compared to neat HDPE and small particle size with low concentration. By adding filler, it restricts the mobility of polymer chain segments and molecules, raising the breakdown temperature and increasing the thermal stability of HDPE/GNP composite. It might be attributed by the introduction of GNP into the polymer, which increases the free volume, is associated with the gap formation between the HDPE chains [17]. The inclusion of GNP is thought to improve the thermal stability of composite materials by preventing the polymer from degrading at early stage when heated. Furthermore, the weight loss of composite was significantly influenced by the decomposition temperature and GNP loading. In the case of G3, there was an observed decrease of about 8% in weight loss as the filler loading increased from 8 wt% to 15 wt%. This suggests that the low weight loss observed can be attributed to the high concentration of filler in the material.

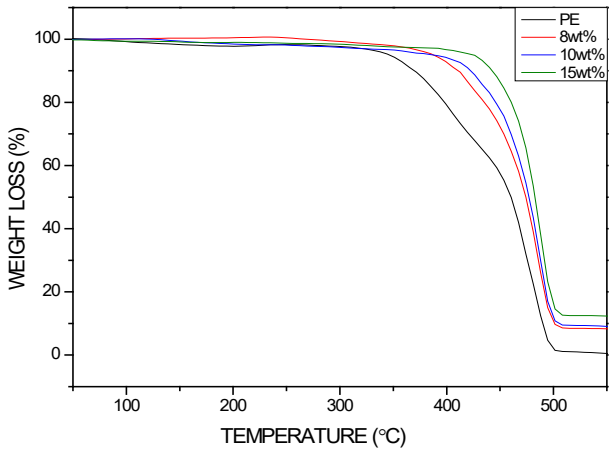

Fig. 1. Mass loss curve of 15um HDPE/GNP with added GNP.

Table 2. Thermal decomposition parameters for HDPE/GNP with added GNP.

Samples	Thermal Degradation Temperature (T_d) (°C)	Total Mass Loss (%)
HDPE	300-500	99.15
8 wt%_G1	300-500	92.74
10wt%_G1	310-500	89.93
15wt%_G1	320-500	85.59
8 wt%_G2	330-500	91.57
10wt%_G2	350-500	91.07
15wt%_G2	380-500	87.49
8 wt%_G3	360-500	93.56
10wt%_G3	380-500	89.04
15wt%_G3	400-500	85.60

3.2. FTIR analysis of GNP/HDPE

Fourier transform infrared spectroscopy (FTIR) investigation is an important tool to define the development of new or disappearance of functional groups. According to Figure 2, the characteristic absorption peaks of HDPE/GNP nanocomposites were mostly concentrated at 2914 cm^{-1}, 2847 cm^{-1}, 1461 cm^{-1}, and 717 cm^{-1}. The peaks at 2847 cm^{-1} are caused by the stretching vibrations of aliphatic C-H bonds, the absorption bands at 1461 cm^{-1}, and 717 cm^{-1}, correspond to the vibrations of benzene rings and their substituents, and 717 cm^{-1} corresponds to the fingerprint absorption peak of HDPE [18]. Alkyl groups are represented by the region of absorption between 2850 and 3000 cm^{-1}. Bands at 2914 cm^{-1} and 2847 cm^{-1} belong to CH_2 groups with strong intensities

and have asymmetric and symmetric stretching, respectively. The CH_2 group's bending mode is primarily responsible for polyethylene's strong band at approximately 1461 cm^{-1}. The medium intensity rocking deformation mode of the CH_2 group is assigned to 717 cm^{-1}. Whilst the GNP, a typical inorganic filler, be added into the matrix would greatly diminish the intensity of the absorption peaks induced by the C-H bond, meanwhile neat HDPE had relatively greater absorption peaks due to the more sensitive reaction of HDPE as an organic in the spectrum. After adding the appropriate amount of GNP, it can be seen that no obvious change at absorption peaks in the HDPE material appeared. Only individual characteristic peak intensities varied, indicating that the GNP in HDPE matrix mainly produced physical modification, thus enhancing the properties of the composite [19]. When the concentration of GNP increased, the relative intensity of peaks associated with CH_2 stretching steadily reduced. The two distinct peaks occur in the spectrum at 2914 cm^{-1} and 2847 cm^{-1} are connected to the CH_2 tensile vibrations which are typical of polyethylene acrylic chains [20]. The observed differences in absorption spectra intensity suggest that HDPE molecules are chemically bonded to the graphene surface, indicating an attachment between the two entities. These findings revealed that there was no complexation in the composites and demonstrated GNP and HDPE interacted well, with good GNP dispersion in the polymer blend.

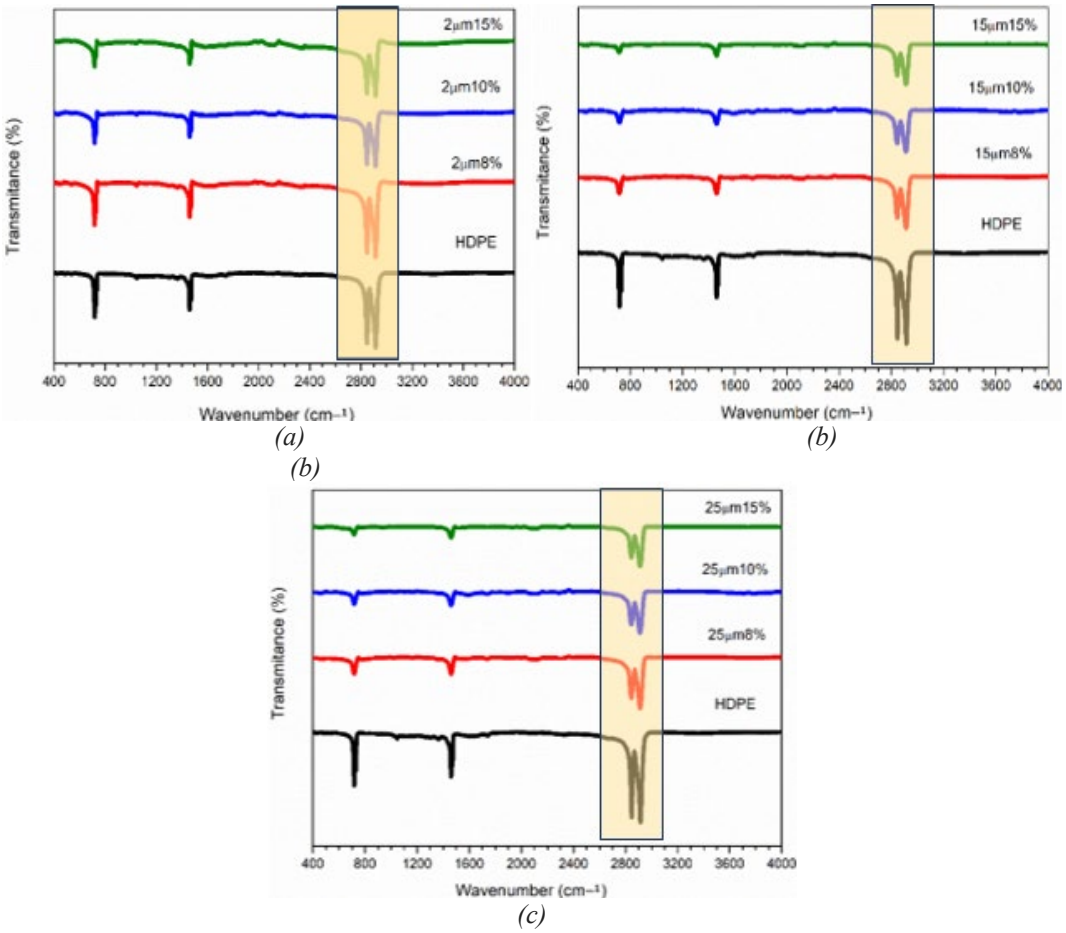

Fig. 2. FTIR spectrum of HDPE/GNP nanocomposites: (a) G1, (b) G2, (c) G3.

Table 3. Intensity and assignment of HDPE/GNP nanocomposites.

Wavenumber (Cm^{-1})	**Assignment**	**Intensity**
2914	CH_2 Asymmetric Stretching	Strong
2847	CH_2 Asymmetric Stretching	Strong
1461	CH_2 Vibration	Medium
717	CH_2 Rocking	Medium

3.4. Electrical conductivity

For the traditional percolation theory of highly dispersive conductive additives in an isolating polymer matrix, the electric fillers can form transfer chains in the bulk of the matrix thus causing the decrease of the resistivity when the content of the conductive additive reaches the percolation threshold [23]. Table 4 reveals that the conductivity value of HDPE/GNP nanocomposite is increasing with increasing the GNP loading. It can be observed that the blending protocol affect the electrical properties and showing good dispersion of the GNP into the matrix of HDPE. The higher conductivity observed in 15 wt % sample is due to the superior dispersion of GNP, which results in greater conductivity. By incorporating GNP as a filler in the HDPE/GNP composite, the resulting interpenetrating network of graphene and polymer leads to a significant enhancement of its electrical conductivity. This improvement can be attributed to the covalent bonding of the large GNP particles, which minimizes contact resistance even at curved regions, ultimately boosting the overall conductivity of the composite [24]. Multiple factors contributing to the enhancement in conductivity of HDPE nanocomposites with an increase in GNP loading [25]. One key factor is the high conductivity of GNP at higher concentrations, which leads to improved networking for electrical conduction. Furthermore, an increase in physical contact between the dispersed GNP-HDPE chains promotes the formation of a conductive network within the nanocomposites. This network facilitates the movement or direct jumping of electrons between conductive materials, thereby boosting the conductivity of the nanocomposites. The improved conductivity in HDPE/GNP nanocomposites can be attributed to an increase in the amorphous regions of the composite material [26]. The addition of GNP to the HDPE matrix enhances the amorphous phase of the polymer host, facilitating the charge-transfer mechanism and promoting rapid conductivity enhancement in the material.

Table 4. Electrical Conductivity HDPE/GNP nanocomposites.

Sample	Electrical Conductivity (S cm^{-1})
8 wt%_G1	4.4×10^{-12}
10wt%_G1	4×10^{-12}
15wt%_G1	3.7×10^{-12}
8 wt%_G2	3.7×10^{-12}
10wt%_G2	6×10^{-10}
15wt%_G2	1.62×10^{-06}
8 wt%_G3	2.8×10^{-12}
10wt%_G3	3.2×10^{-12}
15wt%_G3	1.1×10^{-09}

3.5. Mechanical properties

3.5.1. Tensile test

Young's modulus is an important measure of stiffness, and it is predicted to remain independent of the concentration of GNP during fracture stress. Figure 3 demonstrates that Young's modulus increases in a linear fashion with the concentration of GNP, highlighting the potential for GNP to enhance the mechanical properties of composites. The increase in the modulus of the

composite material is attributed to the good dispersion of nanocarbon in the HDPE matrix, which results in a strong interfacial area between the particles and the matrix [27]. GNP-based composites have demonstrated better reinforcement with a linear increase in concentration, indicating their effectiveness as functional modifiers. The small size and high surface area of GNP allow it to disperse well within the polymer matrix, resulting in improved properties. The high aspect ratio of GNP allows for better intercalation and interface bonding with the polymer matrix, further contributing to the improved reinforcement in GNP-based nanocomposites. The Young's modulus exhibits a superlinear increase with filler concentration, indicating accelerated stiffening, with an additional enhancement observed at higher GNP loadings. This enhancement is likely due to the good distribution and interfacial adhesion between the HDPE matrix and the fillers, which enables better load transfer from the matrix to the fillers [28]. However, the degree of GNP exfoliation within the polymer matrix can affect the value of Young's modulus, with exfoliation levels changing slightly as filler loading increases. At low concentrations of GNP, the value of Young's modulus may be lower due to reduced exfoliation in the elastic zone of the specimen [29]. This phenomenon is observed in composites with a loading of 8 wt% HDPE/ GNP, where the value of Young's modulus is lower.

The increasing of filler concentration in polymer composite leads to an increase in Young's modulus, which indicates an additional enhancement in the material's mechanical properties [16]. This behaviour is due to effective stress transfer between the matrix and filler, resulting from the uniform dispersion of nanoplatelets. However, further addition of GNP into the polymer may lead to restacking of the nanoplatelets due to van der Waals attraction between them. The interlocking between the matrix and the reinforcement contributes to the composites being more rigid after the reinforcement is added [30]. This could also be due to overlapping of GNP with each other and the strong pi–pi attractions between graphene sheets. Such improvement in the mechanical behaviour of composites is attributed to the high strength and excellent adhesion of GNP with matrix particles, which resist rupture and phase separation, preventing dislocation motion across the matrix-reinforcement interface. The composites containing GNP exhibit better mechanical properties, with the specific grade and particle size of the GNP affecting the overall performance [31]. Factors such as the graphene structure, fabrication technique, dispersion of fillers in the matrix, filler orientation, and the interaction between filler and matrix all significantly influence the mechanical and functional properties of graphene nanocomposites. The excellent mechanical properties of GNP make them an effective filler material for composites. GNP act as a bridging filler, linking up crack surfaces to resist crack propagation. This is due to the higher inherent mechanical properties of GNP, which prevent a reduction in breaking strain even when fillers agglomerate during the elongation of the composite [32]. Despite these variations in Young's modulus, the use of GNP-based nanocomposites shows great promise for improving the mechanical properties of composites.

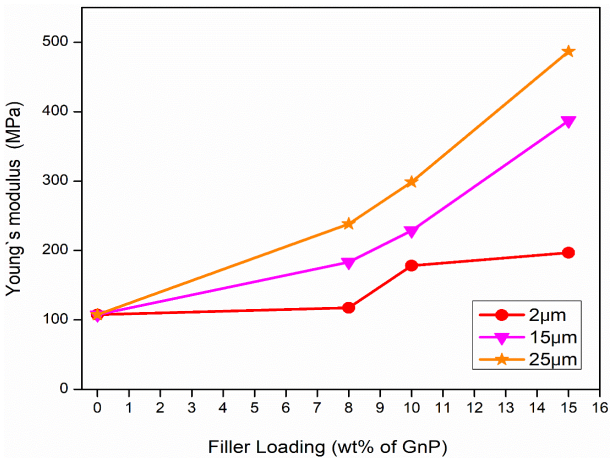

Fig. 3. Young`s modulus of HDPE/GNP nanocomposites.

3.5.2. Impact test

The dispersion status of various loadings can lead to varying energy-absorbing mechanisms at the fracture surface upon impact. The sudden decrease in impact strength is attributed to the restacking of graphene, which is caused by the van der Waals force between the nanoplatelets. When subjected to tensile testing, the stacked graphene sheets may slide, resulting in a less effective reinforcement of strength. In Figure 4, the impact strength of HDPE/GNP composites reduces as the GNP loading increases. Notably, the composites containing 15 wt% of nanofillers exhibit a more significant decline in impact strength compared to those with 8 wt% and the plain HDPE samples. This decrease in impact strength could be due to potential incompatibility between the matrix and filler, as well as the heterogeneous nature of the composites [33]. At low concentrations, GNP are uniformly dispersed in the HDPE matrix and improve toughness by absorbing impact energy [34]. However, as GNP concentration increases, movement of polymer chains is restricted, leading to a reduction in impact strength for HDPE/GNP nanocomposites. Similarly, poorly dispersed GNP in HDPE/ GNP nanocomposites decreases impact strength due to matrix cracking and localized stress. Due to their inherent rigidity, the inclusion of graphene nanoplatelets in the composite resulted in a notable reduction in its toughness [35]. Strong covalent bonding between nanofillers and the matrix enhances a material's performance by increasing its ability to withstand force before breaking [36]. However, excessive GNP loading can cause poor dispersion, leading to nanofiller clustering, resulting in lower impact resistance and brittle behaviour.

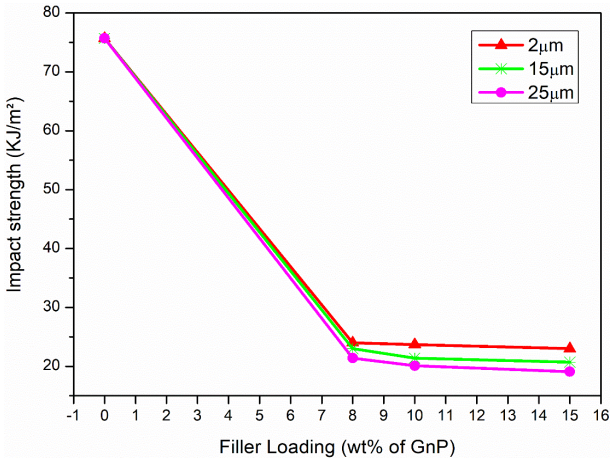

Fig. 4. Impact strength of HDPE/GNP nanocomposites.

3.6 SEM micrograph

The dispersion of graphene platelets (GNP) in HDPE matrix was examined using scanning electron microscopy (SEM). Figure 5 shows SEM micrographs of the tensile fracture surface G2 sample of 8, 10, and 15 wt% HDPE/GNP composites. Figure 5a shows the morphology of fracture at high magnification, confirming the strong attachment of GNP to the HDPE matrix during the mixing process. The surface of HDPE/ GNP displays a conspicuous roughness that may be attributed to the uniform dispersion of GNP in the HDPE matrix. The fracture morphology confirms the tensile and impact strength results in Figure 5, where the 8 wt%_G2 sample shows high ductility, and the 15 wt%_G2 nanocomposite has high reinforcement efficiency with a high Young's modulus, highly brittle, and low energy fracture surface. The rough surface with less GNP loading shows remarkable toughness fracture features, and GNP could be well-dispersed and embedded in the HDPE matrix, resulting in improved interfacial adhesion with less voids [39]. The surface shows that the material absorbs energy yet results in ductile fracture surfaces [40]. The platelets begin to overlap on one another at higher loading, as illustrated in Figure 5b. Agglomerated GNP can be seen in Figure 5c corresponding to a fully stacked GNP due to van der Waals forces and π–π attraction, which are the main bane to GNP' dispersion in polymer matrix. This corresponds to 15 wt% loading in which case

the impact strengths have declined. In Figure 5c, the relatively voids surface fracture morphology indicates a typical fractographic feature of brittle fracture behaviour. The fracture is very brittle, and it is evident that the material rapidly released strain energy to fracture resulting from GNP agglomerates and the absence of cracks or voids. The presence of voids increases matrix viscosity, leading to the formation of more voids [42]. These defects lead to a significant decrease of compressive strength. A reduction of the mechanical properties due to the formation of agglomerates at higher loading ratios could be possible, probably due to GNP self-agglomeration with loading [43]. The clustering of GNP at a loading of 15 wt% is expected to have an adverse impact on the adhesive forces between the matrix and particles and composition. In other words, the increased agglomeration of GNP is likely to weaken the bonding between the matrix and particles. The two-dimensional geometry of graphene nanoplatelets (GNP) in polymer/graphene nanocomposites makes them more resistant to load sharing and crack propagation compared to spherical particles. As the loading of GNP in the matrix increases, they may stack and behave like graphite, which can be easily peeled off under loading [45].

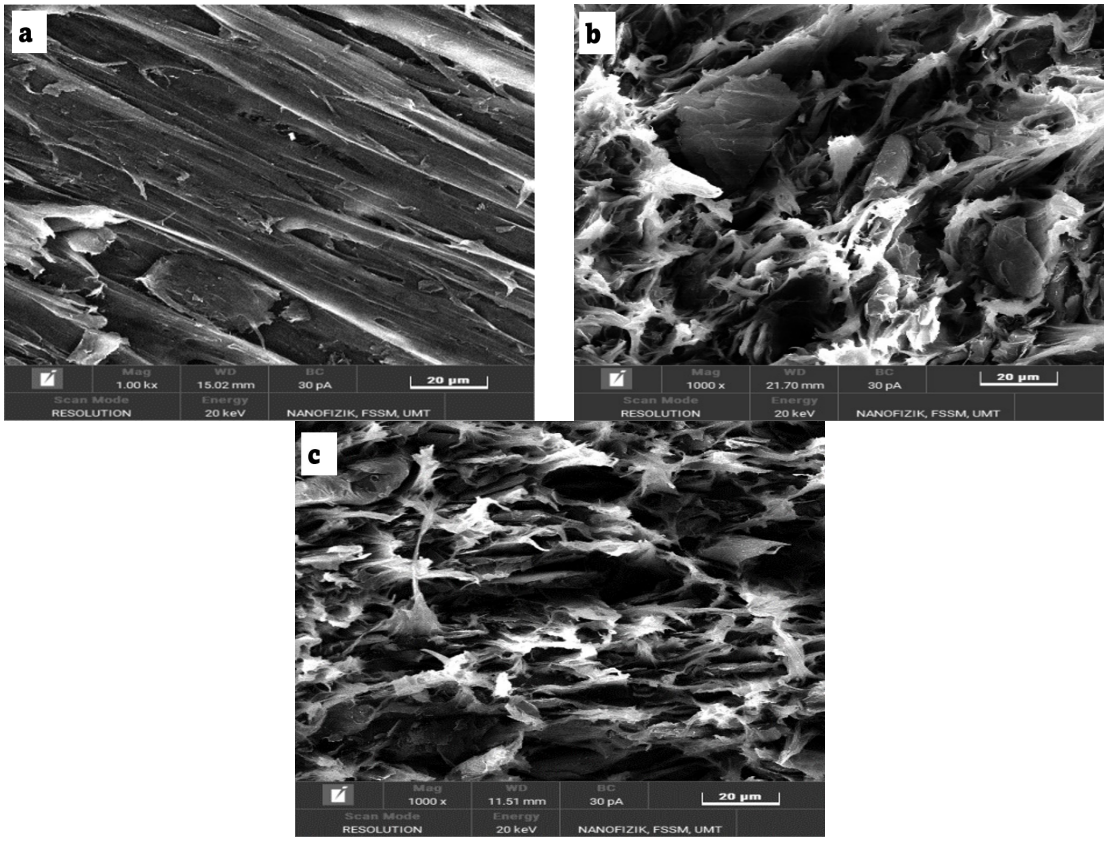

Fig. 5. SEM micrographs of 15 µm HDPE/GNP nanocomposites: (a) 8 wt%_G2, (b) 10wt%_G2, (c) 15wt%_G2.

4. Conclusion

The study involved preparing HDPE-based nanocomposites using three types of GNP, namely G1, G2, and G3, which differed in terms of their lateral sizes and compositions. A melt mixing method and injection moulding were employed in the preparation process. The FTIR findings indicated that GNP' addition affected the reflection peaks and peak intensities, leading to slight differences in the FTIR spectra of the nanocomposites compared to pure HDPE. SEM images revealed that GNP with lower compositions exhibited uniform and random dispersion in the HDPE matrix, with 8 wt% showing more GNP pathways, while 15 wt% displayed a worse distribution than

the others. The lateral size of the GNP was more critical than their compositions in enhancing the nanocomposites' thermal and electrical conductivity. The 15wt%_G3 nanocomposite displayed the highest thermal stability and electrical conductivity among all the HDPE/GNP nanocomposites. An optimal composition was required to achieve the highest electrical and thermal conductivities for a fixed lateral size.

The percolation threshold varied significantly with the size and composition of the GNP, with 8 wt%_G1 exhibiting the lowest percolation threshold. Furthermore, it was found that G1 series exhibited the lowest enhancement of the Young's modulus due to worse distribution in the HDPE matrix and a less effective stress transfer between HDPE and GNP. However, G1 had the highest impact strength compared to G2 and G3 due to the strong covalent bonding between nanofillers and the matrix. Based on all the experimental measurements, it was concluded that G3 series (having a larger lateral size) was the most favourable type of GNP for achieving the best enhancement of nanocomposite properties.

Acknowledgements

The research was supported by the Ministry of Higher Education (MOHE) of Malaysia through the Fundamental Research Grant Scheme (FRGS/1/2020/STG05/UMT/03/2). The authors acknowledge the Faculty of Science and Marine Environment, Universiti Malaysia Terengganu for providing technical supports.

References

[1] Seretis, G., D. Manolakos, and C. Provatidis, Composites Part B: Engineering, **145**, 81 (2018); https://doi.org/10.1016/j.compositesb.2018.03.020.
[2] Novoselov, K.S., A.K. Geim, S.V. Morozov, D.-e. Jiang, Y. Zhang, S.V. Dubonos, I.V. Grigorieva, and A.A. Firsov, 306(5696) 666 (2004); https://doi.org/10.1126/science.1102896.
[3] Owida, H.A., N.M. Turab, and J. Al-Nabulsi, Bulletin of Electrical Engineering Informatics, 12(2) 891 (2023) https://doi.org/10.11591/eei.v12i2.4310.
[4] Yang, H., D. Zheng, W. Tang, X. Bao, and H. Cui, Journal of Building Engineering, 105721 (2022); https://doi.org/10.1016/j.jobe.2022.105721.
[5] Nassiet, V., B. Hassoune-Rhabbour, O. Tramis, and J.-A. Petit, Electrical and electronics, in Adhesive Bonding, Elsevier, UK, 719 (2021)
[6] Antunes, M., G. Gedler, H. Abbasi, and J.I. Velasco, Materials Today: Proceedings, **3,** S233 (2016); https://doi.org/10.1016/j.matpr.2016.02.039.
[7] Jiménez-Suárez, A. and S. Prolongo, Applied Sciences **10**(5) 1753 (2020); https://doi.org/10.3390/app10051753.
[8] Tiwari, S.K., S. Sahoo, N. Wang, and A. Huczko, Journal of Science: Advanced Materials Devices, **5**(1) 10 (2020); https://doi.org/10.1016/j.jsamd.2020.01.006.
[9] Lee, D.-K., J. Yoo, H. Kim, B.-H. Kang, and S.-H. Park, Materials, **15**(4) 1356 (2022) https://doi.org/10.3390%2Fma15041356.
[10] Alemour, B., M. Yaacob, H. Lim, and M.R. Hassan, International Journal of Nanoelectronics & Materials, **11**(4) (2018).
[11] Demski, S., K. Dydek, K. Bartnicka, K. Majchrowicz, R. Kozera, and A. Boczkowska, Polymers, **15**(3) 506 (2023); https://doi.org/10.3390/polym15030506.
[12] Mahmoud, M.E., M.A. Khalifa, M.R. Youssef, and R.M. El-Sharkawy, Journal of Applied Polymer Science, **139**(31) e52705 (2022); https://doi.org/10.1002/app.52705.
[13] Zhou, S., A.N. Hrymak, and M.R. Kamal, Composites Part A: Applied Science and Manufacturing, **103,** 84 (2017); https://doi.org/10.1016/j.compositesa.2017.09.016.
[14] Al-Maqdasi, Z., G. Gong, B. Nyström, N. Emami, and R. Joffe, Materials, **13**(9) 2089 (2020) https://doi.org/10.3390/ma13092089.
[15] Alam, F.E., J. Yu, D. Shen, W. Dai, H. Li, X. Zeng, Y. Yao, S. Du, N. Jiang, and C.-T. Lin, Polymers, **9**(12) 662 (2017); https://doi.org/10.3390/polym9120662.

[16] Boudjellal, A., D. Trache, S. Bekhouche, A. Abdelaziz, M.S. Razali, S. Touidjine, and K. Khimeche, Materials Letters, 289, 129379 (2021); https://doi.org/10.1016/j.matlet.2021.129379
[17] Mohammed, Z., A. Tcherbi-Narteh, and S. Jeelani, SN Applied Sciences, **2**, 1959 (2020); https://doi.org/10.1007/s42452-020-03780-1.
[18] Ingavale, R. and P. Raut, Nature Environment and Pollution Technology, **17**(2) 649 (2018).
[19] Zhou, H.-Y., H.-B. Dou, and X.-H. Chen, Materials, **14**(14) 3986 (2021); https://doi.org/10.3390/ma14143986.
[20] Hashemi, M., A. Rostami, I. Ghasemi, and A. Omrani, Journal of Polymers and the Environment, 31, 27151 (2023); https://doi.org/10.1007/s10924-022-02701-0.
[21] López-González, M., A. Flores, F. Marra, G. Ellis, M. Gómez-Fatou, and H. J. Salavagione, Polymers, **12**(9) 2094 (2020) https://doi.org/10.3390/polym12092094.
[22] Krupa, I., V. Cecen, A. Boudenne, J. Prokeš, and I. Novák, Materials & Design, **51**, 620 (2013); http://dx.doi.org/10.1016/j.matdes.2013.03.067.
[23] Liu, F., X. Zhang, W. Li, J. Cheng, X. Tao, Y. Li, and L. Sheng, Composites Part A: Applied Science and Manufacturing, **40**(11) 1717 (2009); https://doi.org/10.1016/j.compositesa.2009.08.004.
[24] Tarannum, F., S. Danayat, A. Nayal, R. Muthaiah, R.S. Annam, and J. Garg, Materials Chemistry and Physics, 289, 127404 (2023); https://doi.org/10.1016/j.matchemphys.2023.127404.
[25] Pang, A.L., M.R. Husin, A. Arsad, and M. Ahmadipour, Journal of Materials Science: Materials in Electronics, **32**, 9574 (2021); https://doi.org/10.1007/s10854-021-05620-3.
[26] Al-Muntaser, A., R.A. Pashameah, E. Alzahrani, S.A. AlSubhi, S. Hameed, and M. Morsi, Journal of Polymers and the Environment, 31, 2534 (2023); https://doi.org/10.1007/s10924-022-02748-z.
[27] Segun, A., B.O. Adewuyi, D.O. Ojo, and O.N. Gideon, Journal of Physical Science, **32**(2), 41 (2021); https://doi.org/10.21315/jps2021.32.2.4.
[28] Wijerathne, D., Y. Gong, S. Afroj, N. Karim, and C. Abeykoon, Journal of Lightweight Materials and Manufacture, **6**(1) 117 (2023); https://doi.org/10.1016/j.ijlmm.2022.09.001.
[29] Spinelli, G., R. Guarini, R. Kotsilkova, T. Batakliev, E. Ivanov, and V. Romano, Materials, **15**(3) 986 (2022); https://doi.org/10.3390/ma15030986.
[30] Rashad, M., F. Pan, Z. Yu, M. Asif, H. Lin, and R. Pan, Progress in natural science: materials international, **25**(5) 460 (2015); http://dx.doi.org/10.1016/j.pnsc.2015.09.005.
[31] Seo, J.-S., D.-H. Kim, H.-S. Jung, H.-D. Kim, J. Choi, M. Kim, S.-H. Baeck, and S.-E. Shim, Polymers, **14**(18) 3824 (2022); https://doi.org/10.3390/polym14183824.
[32] Iqbal, A.A., N. Sakib, A.P. Iqbal, and D.M. Nuruzzaman, Materialia, **12,** 100815 (2020); https://doi.org/10.1016/j.mtla.2020.100815.
[33] Inuwa, I., A. Hassan, S. Samsudin, M.M. Haafiz, M. Jawaid, K. Majeed, and N.A. Razak, Journal of Applied Polymer Science, **131**(15) 40582 (2014); https://doi.org/10.1002/app.40582.
[34] Wang, L., J. Hong, and G. Chen, Polymer Engineering & Science, **50**(11) 2176 (2010); https://doi.org/10.1002/pen.21751.
[35] Wang, Q., Y. Wang, Q. Meng, T. Wang, W. Guo, G. Wu, and L. You, RSC advances, **7**(5) 2796 (2017); https://doi.org/10.1039/C6RA26458A.
[36] Hussein, S.I., A.M. Abd-Elnaiem, T.B. Asafa, and H.I. Jaafar, Applied Physics A, **124,** 475 (2018); https://doi.org/10.1007/s00339-018-1890-0.
[37] Shivakumar, H., N. Renukappa, K. Shivakumar, and B. Suresha, Open Journal of Composite Materials, **10**(02) 27 (2020); https://doi.org/10.4236/ojcm.2020.102003.
[38] Wakabayashi, K., C. Pierre, D.A. Dikin, R.S. Ruoff, T. Ramanathan, L.C. Brinson, and J.M. Torkelson, Macromolecules, **41**(6) 1905 (2008) https://doi.org/10.1021/ma071687b.
[39] Ma, J., Q. Meng, I. Zaman, S. Zhu, A. Michelmore, N. Kawashima, C.H. Wang, and H.-C. Kuan, Composites Science and Technology, **91**, 82 (2014); http://dx.doi.org/10.1016/j.compscitech.2013.11.017.
[40] Sultana, S.N., E. Helal, G. Gutiérrez, E. David, N. Moghimian, and N.R. Demarquette, Crystals, **13**(2) 358 (2023); https://doi.org/10.3390/cryst13020358.
[41] Scariot, M.A., B.R. Fenner, M. Beltrami, L.V. Beltrami, and A.J. Zattera, Iranian Polymer Journal, **32**(1) 59 (2023); https://doi.org/10.1007/s13726-022-01101-4.

[42] Mannov, E., H. Schmutzler, S. Chandrasekaran, C. Viets, S. Buschhorn, F. Tölle, R. Mülhaupt, and K. Schulte, Composites Science and Technology, **87**, 36 (2013) https://doi.org/10.1016/j.compscitech.2013.07.019.
[43] Zhuang, Y., X. Cao, J. Zhang, Y. Ma, X. Shang, J. Lu, S. Yang, K. Zheng, and Y. Ma, Composites Part A: Applied Science and Manufacturing, **120**, 49 (2013); https://doi.org/10.1016/j.compositesa.2019.02.019.
[44] Abbass, A., M.C. Paiva, D.V. Oliveira, P.B. Lourenço, and R. Fangueiro, Composites Part A: Applied Science and Manufacturing, **166**, 107379 (2023); https://doi.org/10.1016/j.compositesa.2022.107379.
[45] Mabaya, M., R. Aguiar, H. Costa, A. de Barros, J. Reis, and J. Souza, International Journal of Adhesion and Adhesives, **122**, 103317 (2023); https://doi.org/10.1016/j.ijadhadh.2022.103317.